SELF- AND IMPURITY DIFFUSION IN INTRINSIC RELAXED SILICON - GERMANIUM

BY
PAULI LAITINEN

DEPARTMENT OF PHYSICS
UNIVERISTY OF JYVÄSKYLÄ

ISBN 978-951-39-3150-6

URN:ISBN:978-951-39-3150-6

TABLE OF CONTENTS

1 INTRODUCTION 3

2 PURPOSE AND STRUCTURE OF THIS STUDY 6

3 DIFFUSION IN SEMICONDUCTORS 8

3.1 General considerations and theory of diffusion 8
3.2 Diffusion mechanisms in semiconductors 10
3.2.1 Interstitial mechanism 10
3.2.2 Interstitialcy mechanism 10
3.2.3 Vacancy mechanism 11
3.2.3 Kick-out and dissociative mechanisms 12
3.2.4 Other diffusion mechanisms 13
3.3 Diffusion under equilibrium and non-equilibrium conditions -concentration of point defects 14
3.4 Diffusion via defects in semiconductors 18

4 EXPERIMENTAL METHODS FOR SOLID-STATE DIFFUSION 22

4.1 Conventional techniques 22
4.2 Diffusion studies by the modified radiotracer technique 25
4.2.1 Radiotracer production and deposition 25
4.2.2 Diffusion annealing 28
4.2.3 Serial sectioning by sputtering 29
4.2.4 Activity measurement and profile construction 31
4.2.5 Analysis of the experimental depth profile 32

5 DIFFUSION IN SIGE 35

5.1 Self- and impurity diffusion in Si and Ge 35
5.1.1 Si self-diffusion 35
5.1.2 Impurity diffusion in Si 38
5.1.3 Self- and impurity diffusion in Ge 41
5.2 Self- and impurity diffusion in SiGe 43
5.2.1 SiGe self-diffusion 43
5.2.2 Impurity diffusion in SiGe 45

SUMMARY 50

REFERENCES 51

1 Introduction

Diffusion in general is present in most dynamical processes in the nature. Diffusion is pronounced especially at high temperatures and it exists in all forms of matter. Diffusion plays significant role for example in corrosion of metals and nutrition of human cells. Considering the generality and variety of diffusion processes, it is clear that understanding and controlling the diffusion has great importance for science, technology as well as for economy.

It can be claimed that Roberts and Austen started solid-state diffusion research already in 1896. Many diffusion studies were performed in 1930´s [Meh36], but it was the invention of the transistor in 1948 by Bardeen, Brattain and Schockley [Sch49], which gave a boost for the diffusion research. The need for controllable doping of semiconductors was apparent and this required information on diffusion of dopant atoms and their coupling with defects acting as diffusion vehicles. The diffusion in semiconductors has remained a challenge to physicists as the list of novel semiconductors grows and yet many basic issues are still unsolved.

Silicon-Germanium (SiGe) alloy is a compound semiconductor, whose constituents Si and Ge are the best-known semiconductors. Si is the most studied elemental semiconductor, since it is still the material used in over 90% of the electronic devices [Pau00]. The first transistors, on the other hand, were based on Ge. It was later changed to Si due larger band gap of Si and better insulation properties of SiO_2 over GeO_2.

The first SiGe studies were conducted already in 1956 by Glickman, who measured the magnetoresistance in polycrystalline SiGe [Gli55]. This material was soon abandoned due to its too poor quality to be used for electronic device applications. The rediscovery of SiGe occurred in late 1970´s, when Kasper (1975) found the way to grow single crystalline SiGe-layers by molecular beam epitaxy (MBE) [Kas75]. Ever since SiGe has been on stage for device development and as an active research topic.

The SiGe material can be divided into two categories: strained and relaxed. The lattice parameter of Ge crystal is 4% larger than of Si. Relaxed $Si_{1-x}Ge_x$ compound has a lattice parameter value between those of Si and Ge and it depends on composition x [Dis64]. When growing SiGe epi-layer on a Si-substrate, the SiGe adopts the lattice constant of Si introducing strain to the SiGe layer. When a certain critical thickness of the epi-layer is exceeded, the strained SiGe crystal relaxes to its natural size via forming high concentration of dislocations (~10^{10}-10^{11} cm^{-2}) [Nyl00] in the Si-SiGe interface [Peo85, Peo86]. Similar to the growth of lattice mismatched III-V compounds [Abr75], the high quality relaxed SiGe epi-layers can be grown on Si by using buffer layers. These epitaxial SiGe layers are grown on Si-wafers by increasing gradually the Ge-content, when dislocations relax the strain. On this buffer layer a relaxed high quality single crystal SiGe layer can be grown. Employing the modified MBE or chemical vapor deposition techniques with varying growth conditions a relaxed $Si_{1-x}Ge_x$ layer with any composition ($0 \leq x \leq 1$) can be grown having dislocation densities in the order of 10^6 cm^{-2} and below [Nyl00, Ros00]. High quality bulk SiGe has been also grown by the Czochralski method in the composition ranges $x < 0.15$ and $x > 0.85$ [Yon99] and by the float zone method with $x < 0.054$ [Wol96] and by the liquid encapsulated zone melting method with $x > 0.95$ [Bli97]. By optimizing the growth method the bulk composition of SiGe has been extended to $x \geq 0.78$ [Azu03], but bulk relaxed SiGe within the full composition range is not yet available. Although the quality of SiGe has improved over the years it is still a limiting factor for device processing applications [Pau00].

The great potential of SiGe for technology arises from the possibility to modify its properties by altering the composition. For example, the band gap decreases from 1.1 eV (pure Si) to 0.65 eV (pure Ge) at room temperature and its structure stays Si-like up to composition x= 0.85 and then changes Ge-like [Web95]. The band gap can also be tailored by strain [Fro95]. By building different kinds of Si-SiGe heterostructures various properties for device design can be optimised. An excellent example of this is the hetero bipolar transistor [Pru92], which has superior performance, compared to conventional Si-based devices [Pau00, Xie99].

SiGe has also great economical potential, since the production of SiGe-devices is highly compatible with conventional Si-technology. This means that SiGe-technology can be adopted aside with existing Si-technology without enormous economical input. The cost is the main reason why many novel compound semiconductors, though with superior performance compared to Si, have failed to challenge the dominance of silicon in electronic device markets.

The SiGe-substrate offers also an excellent playground for basic physics research. SiGe is particularly interesting for diffusion and defect studies, which are closely related, as will be seen later in section 3. Defect studies in SiGe can yield information on similar defects in Si [Mes03]. SiGe has also shown to be a good platform for strain effect studies [Azi99, Cow94, Zan01]. By studying the self- and dopant diffusion in relaxed SiGe as a function of composition knowledge on thermodynamics of defects and impurity atoms can be obtained. This helps us to understand the properties of the alloying effect and get more insight into the properties of Si and Ge elements itself.

2 Purpose and structure of this study

The purpose of this study is to determine experimentally the diffusion properties of self- and dopant atoms in intrinsic relaxed SiGe and study their dependency on SiGe composition. Thesis also includes device development for diffusion studies by the modified radiotracer technique.

The content of this thesis is the following: in section 3 basic theories and concepts for diffusion in semiconductors are introduced. In the following section (4) the applied experimental technique is presented together with a short review of other relevant techniques to performing experimental diffusion studies in semiconductors. The last section (5) begins with a review of diffusion in Si and Ge. Rest of that section is devoted to showing the present picture of diffusion in relaxed intrinsic SiGe in the light of the experimental results, including the author's work, and theoretical calculations existing so far.

This thesis is based on the following publications. The articles are referred with Roman numerals in the text.

I P. Laitinen, G. Tiourine, V. Touboltsev, J. Räisänen, *Detection system for depth profiling of radiotracers,* Nuclear Instruments and Methods in Physics Research, Section B **190**, 183 (2002).

II P. Laitinen, M. Nevala, A. Pirojenko, K. Ranttila, R. Seppälä, I. Riihimäki, J. Räisänen A. Virtanen, *Utilisation of a sputtering device for targetry and diffusion studies*, submitted to Nuclear Instruments and Methods in Physics Research, Section B.

III A. Strohm, T. Voss, W. Frank, P. Laitinen, J. Räisänen, *Self-diffusion of ^{71}Ge and ^{31}Si in SiGe alloys,* Zeitschrift für Metallkunde **93**, 737 (2002).

IV P. Laitinen, A. Strohm, J. Huikari, A. Nieminen, T.Voss, C. Grodon, I. Riihimäki, M. Kummer, J. Äystö, P. Dendooven, J. Räisänen, W. Frank and the ISOLDE Collaboration, *Self-diffusion of ^{31}Si and ^{71}Ge in relaxed $Si_{0.20}Ge_{0.80}$ layers,* Physical Review Letters **89**, 085902 (2002).

V P. Laitinen, I. Riihimäki, J. Räisänen, *Arsenic diffusion in relaxed $Si_{1-x}Ge_x$,* Physical Review B **68**, 155209 (2003).

Author's contribution in the articles:

The author has been responsible for planning, developing and testing the devices presented in articles I and II. The author has realized most of the experiments and data analysis for articles IV and V and participated in measurements and data analysis of the article III. The author has written the first versions of articles I, II, IV and V and participated in writing of article III.

3 Diffusion in semiconductors

3.1 General considerations and theory of diffusion

Diffusion in general is the redistribution of particles as a result of random (Brownian) motion. Random motion requires that there are no driving forces of any kind. Diffusion coefficient is defined to describe the magnitude of diffusion per unit time. This coefficient is characteristic for each combination of diffusing particle and media. The definition of diffusion coefficient is given by the general equation for flux of atoms moving through a plane of unit area

$$J(x,t) = -D(x,t)\left(\frac{\partial C(x,t)}{\partial x}\right), \qquad (1)$$

which is known as Fick's first law, where D(x) [m^2/s] is the diffusion coefficient (or often called as diffusivity) and C(x,t) is the concentration of moving atoms [atoms/m^3]. The time dependence of the concentration is given the by Fick´s second law

$$\frac{\partial C}{\partial t} = \frac{\partial}{\partial x}\left(D\frac{\partial C}{\partial x}\right). \qquad (2)$$

If the diffusion coefficient D is constant respect to time, position and concentration, Eq. (2) reduces to

$$\frac{\partial C}{\partial t} = D\left(\frac{\partial^2 C}{\partial x^2}\right). \qquad (3)$$

Eq. (3) is called the concentration independent diffusion equation and it can in some cases be solved analytically. The numerical solution can be applied to any initial profile of arbitrary shape to extract constant D values [Cra75]**.** Determination of D values from

experimental profiles requires that the initial condition for diffusion be well established. Also meaningful boundary conditions need to be included in the analysis.

Sometimes, like in extrinsically doped semiconductors, the D is concentration dependent. In this case the Boltzmann-Matano analyses can be applied to experimental profiles to extract the effective diffusivity D^{eff}. This can also be done by several other more sophisticated numerical methods [Ahl98, Cra75].

The temperature dependence of the diffusion coefficient D has been found to follow, in most cases, the Arrhenius law

$$D = D_0 \exp\left[-\frac{H_a}{kT}\right], \qquad (4)$$

where D_0 and H_a are called the pre-exponential factor and activation enthalpy (or energy if $H_a \approx E_a$), respectively.

3.2 Diffusion mechanisms in semiconductors

In order to get insight into the physics of diffusion, the underlying microscopic mechanisms must be considered. The diffusion mechanisms suggested to exist in perfect single crystalline semiconductors are presented in the following.

3.2.1 Interstitial mechanism

The simplest diffusion mechanism in semiconductors is called interstitial mechanism (Fig. 1), where the diffusing atom jumps from an interstitial site to another (i.e. in the space between lattice atoms). Diffusion via the interstitial mechanism is typically very fast and it is characteristic of very small atoms compared to host lattice atoms (see chapter 5.1.2).

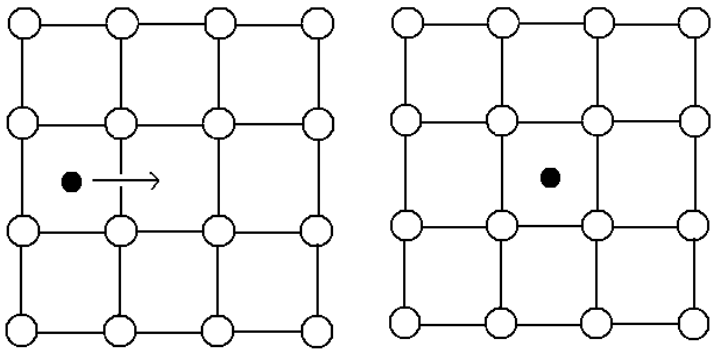

Fig. 1 Interstitial mechanism.

3.2.2 Interstitialcy mechanism

In the interstitialcy mechanism or often referred as interstitial mediated mechanism (Fig. 2), the diffusion proceeds via reaction

$$A_s + I \leftrightarrow A_I, \qquad (5)$$

where A_s is an (self- or impurity) atom at substitutional site and I is the self-interstitial. The substitutional site corresponds to a regular lattice site in the crystal and the self-interstitial is an extra atom occupying the lattice site between ordinary lattice sites in the crystal.

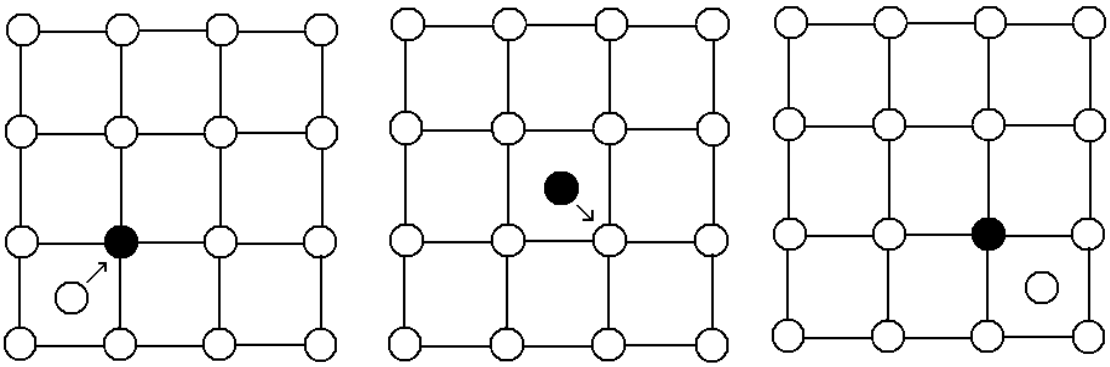

Fig. 2 Interstitialcy mechanism.

In the interstitialcy mechanism atoms dissolved at substitutional sites diffuse by interacting with self-interstitials kicking each other from substitutional sites to interstitial sites.

3.2.3 Vacancy mechanism

The best-known and very common diffusion mechanism is the vacancy mechanism (Fig. 3), which can be described with the reaction

$$A_s + V \leftrightarrow AV, \qquad (6)$$

where V denotes a vacancy defect and AV is the vacancy-atom pair. Vacancy is a void in the ordinary lattice site. In the vacancy mechanism atoms diffuse in the lattice by exchanging places with vacancies.

Similar to the interstitialcy mechanism, substitutionally dissolved atoms need the incorporation of defects in order to diffuse.

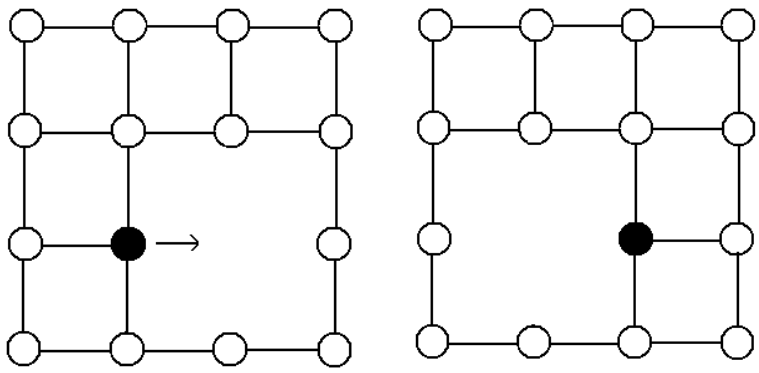

Fig. 3 Vacancy mechanism.

3.2.3 Kick-out and dissociative mechanisms

When the atom can dissolve both to the substitutional and interstitial sites it is possible that the diffusion proceeds via kick-out or dissociative mechanisms.

In the kick-out mechanism the reaction with defects is the same as in the interstitialcy mechanism i.e. the change in lattice site occurs by the kicking between A and I. The difference is that an atom at interstitial (A_I) state can diffuse long distances via direct interstitial mechanism before it is kicked back to a substitutional site according to Eq. 5.

In the dissociative mechanism (also referred as Frank-Turnbull mechanism [Fra56]) the change of the lattice site type occurs via interaction with vacancies according to

$$A_s \leftrightarrow A_I + V. \qquad (7)$$

In other words, the atom in a substitutional site can dissociate to an interstitial site atom and a vacancy (formation of a Frenkel pair) and backward reaction occurs by recombination of the interstitial atom and the vacancy to A_s.

Similar to the kick-out reaction, A_I can diffuse long distances via direct interstitial mechanism before it recombines with a vacancy, to become a substitutional atom.

Characteristics to these two mechanisms are large effective diffusion coefficients, since direct interstitial diffusion is very rapid compared to point defect mediated diffusion (like interstitialcy and vacancy mechanisms). Depending on diffusion circumstances, the kick-out mechanism may be responsible for the extra-ordinary shapes observed in some experimental diffusion profiles. These shapes can be used as an identification of this mechanism. This is a special case since usually it is impossible to deduce the underlying diffusion mechanisms from the shapes of the experimental diffusion profiles alone [Stol83].

3.2.4 Other diffusion mechanisms

Diffusion mechanisms described in Sec. 3.2.1-3 are commonly acknowledged, but there are also other mechanisms that have been proposed to be responsible for the diffusion in semiconductors.

The simplest diffusion step is the direct exchange of two lattice atoms. Glazmann et al. [Gla77] have proposed that the self-diffusion of silicon proceeds by this direct exchange mechanism.

The cousin of the direct exchange mechanism is the more complicated concerted exchange mechanism proposed by Pandey [Pandey86]. In this mechanism the substitutional atoms jump to other substitutional sites by sequence of steps, involving bond braking and rotation.

A recent suggestion as the diffusion vehicle for Si is the so-called fourfold coordinated defect (FFCD), where the diffusion jump can occur by the swing of a special two-atom defect [Goe02].

So far no experimental evidence of mechanisms presented in this section has been found.

3.3 Diffusion under equilibrium and non-equilibrium conditions -concentration of point defects

Diffusion proceeds in semiconductors in most cases by the aid of point defects via mechanisms described in section 3.2. It is evident that diffusion depends strongly on the concentration and mobility (i.e. diffusivity) of these point defects i.e. self-interstitials (I) (Fig. 2) and vacancies (V) (Fig. 3).

The concentration of the point defects in a perfect crystal at thermal equilibrium can be formulated as a perfect dilute solution by the expression

$$C_d^{eq} = \exp\left[\frac{S_d^F}{k} - \frac{H_d^F}{kT}\right], \qquad (8)$$

when formation and annihilation rates of the point defects are equal. In Eq. (8), subscript d represents the defect type (either I or V), S^F and H^F are the entropy and enthalpy of formation, k the Boltzmann constant and T temperature. Parameters S^F and H^F are material dependent, which means that the defect concentration depends on the material, as well as the temperature.

Eq. (8) is determined entirely by the thermodynamics (minimum of the Gibbs free energy) of the point defect formation. It does not tell us how and by which rate this equilibrium concentration is achieved. In order to understand this, the reactions producing and annihilating these defects must be considered. This is required also in order to know under which conditions C_d^{eq} prevails or not.

In perfect crystal point defects can be formed by spontaneous dissociation of substitutional atoms to interstitials (I) and vacancies (V). This process is referred to as formation of Frenkel pairs. Point defects can also be formed when surface atoms migrate into the bulk crystal forming interstitials, or when self-atoms migrate from the bulk to the surface leaving vacancies inside the crystal. These surface-related processes are called Schottky-processes.

Noteworthy is that the formation enthalpy of the defects does not depend on atomistic processes on the surface. The concentration of the defects depends on the bulk properties of the crystal alone [Fah89]. Defect annihilation can occur by their migration to the surface or by I-V recombination.

Real crystals are imperfect and thus several additional processes affect point defect production and annihilation.

Point defect concentration may alter as they interact with extended defects, which always exist in real crystals to some extent. For example dislocations, which consists of a large number of atoms dislocated from their original lattice sites, can act as sources or sinks for point defects. Precipitates start to form when the impurity concentration exceeds the solubility limit in the crystal. Precipitates can act as trapping sites for point defects and they may also change the local crystal density favouring either forming of interstitials or vacancies. Real crystals always contain impurities, but usually the formation of precipitates requires so high impurity atom concentrations, that they must be introduced deliberately into the crystal by doping. If both dislocations and precipitates are present in the crystal, the situation becomes very complex for defect formation. Not only reactions of point defects with both dislocations and precipitates exist, but also interactions between these two: dislocations may act as preferential nucleation sites for precipitates.

The growth conditions of real semiconductor crystals determine the concentration of dislocations and other extended defects as well as the concentration of impurities [Mah00]. These properties in turn affect point defect concentrations and they also have profound effects in device processing, where all reactions mentioned are involved. For example, in silicon both the crystal bulk and its surface are found to act as interstitial sources and their relative contribution depends on the growth method [Fan96].

In the processes described above, the reaction rates are dictated by the thermodynamics and eventually C^{eq} conditions prevail. There are also many processes, which produce excess of defects resulting in defect concentrations that deviate from their equilibrium values (C_d

$\neq C_d^{eq}$). When these processes are active, they have profound effects on the diffusion properties.

Chemical reactions may lead to point defect injection. In silicon, surface oxidation ($Si + O_2 \rightarrow SiO_2$) is known to inject interstitials into silicon, resulting in the super saturation of C_I ($C_I > C_I^{eq}$) and via I-V recombination, the under saturation of C_v ($C_v < C_v^{eq}$). The nitridation ($3Si + 2N_2 \rightarrow Si_3N_4$) of the Si in turn has found to inject vacancies into bulk resulting in the super saturation of C_v and the under saturation of C_I, respectively [Fah89]. The creation of defects due to bombardment with energetic ions, neutrons or electrons is called radiation damage. The concentration and type of defects created depend on the energy deposited to the crystal, i.e. the energy, fluence and type of the radiation [Siz78]. The very rapid cooling of the semiconductor crystal called quenching may also produce excess of point defects as they are frozen before recombination during the cooling process.

After the non-thermal processes producing the point defects have been ended, the equilibrium concentrations of point defects (Eq. (8)) will eventually be reached at a constant temperature. How long this takes, depends on the temperature and how far from equilibrium the defect concentrations are.

The point defects may have several different charge states. The formation enthalpies are different for defects with charge states and the charge state distribution depends on the corresponding electronic energy levels in the band gap. For example, a silicon vacancy has found to have 5 different charge states, from -2 to +2 (V^{--} to V^{++})[Wat00]. Defect studies are usually performed at low temperatures [ICD03] and generally the defect charge state distributions at elevated temperatures are not known. The charge states of defects are especially important when impurity diffusion in semiconductors is concerned, since there may be Coulomb interactions between the defects and impurities. This is dealt in more detail in Sec. 3.4.

Doping has also profound effects on defect concentrations and their charge state distributions. In extrinsically doped semiconductors the concentration of free charge carriers

and thus charged defect concentrations differ from their intrinsic values. Since the neutral defect concentrations are unaffected by the charge carriers and the formation energy of charged defects depend on the Fermi-level, both the total concentration of defects and their charge distribution is changed due to doping. The strength and nature of the doping effects to the defects depend on the dopant atom types and concentrations.

3.4 Diffusion via defects in semiconductors

In section 3.1 general considerations of diffusion and the definition of diffusion coefficient (Eq. (1)) and its temperature dependence (Eq. (4)) were discussed. In section 3.2 the relevant diffusion mechanisms were presented. Now the task is to find the relationship between the atomistic details of the diffusion mechanisms and the diffusion coefficient D.

Let us start by considering the movement of one (tracer) atom. The atom has to jump to a different lattice site. This jump requires overcoming of a certain barrier, which keeps the atoms on their preferential sites in the crystalline lattice. The barrier is denoted by H^m and it is assumed that the energy required overcoming it results from thermal kinetics, i.e. the probability of the diffusion jump depends on temperature. Diffusion via mechanism α can be described as

$$D_\alpha = g_\alpha a_0^2 \nu_{\alpha 0} \exp\left[\frac{S_\alpha^m}{k} - \frac{H_\alpha^m}{kT}\right]. \qquad (9)$$

The equation can be separated as T independent and T dependent parts as

$$D_\alpha = D_{\alpha 0} \exp\left[\frac{-H_\alpha^m}{kT}\right] \qquad (10)$$

with

$$D_{\alpha 0} = g_\alpha a_0^2 \nu_{\alpha 0} \exp\left[\frac{S_\alpha^m}{k}\right]. \qquad (11)$$

In Eq. (9) g_α is the so called geometric factor, which takes into account the geometry of the crystal structure, a_0 is the jump distance and $\nu_{\alpha 0}$ is the attempt frequency, S_α^m and k are the migration entropy and Boltzmann´s constant, respectively. Eq. (9) and (10) describe diffusion via a direct mechanism such as the direct interstitial mechanism (Sec. 3.2).

As described earlier (Sec. 3.2), most of the diffusion mechanisms are indirect requiring interstitials or vacancies to act as diffusion vehicles. This means that the interstitial or vacancy have to first move to vicinity of the diffusing atom in order that the diffusion jump can occur. Once the diffusion jump has occurred, the probability that the jump is cancelled by reverse jump is higher than the probability for another jump, since the defect is still close to the diffusing atom. This effect is called correlation and it has to be taken into account in addition with the defect concentration (Eq. (8)). By combining these three factors we get an expression for tracer atom diffusion via interstitialcy or vacancy mechanism as

$$D = f_\beta D_\beta C_\beta^{eq} = f_\beta g_\beta a_0^2 \nu_{\beta 0} \exp\left[\frac{S_\beta^m}{k} - \frac{H_\beta^m}{kT}\right] \exp\left[\frac{S_\beta^F}{k} - \frac{H_\beta^F}{kT}\right]$$

$$= f_\beta g_\beta a_0^2 \nu_{\beta 0} \exp\left[\frac{S_\beta^F + S_\beta^m}{k}\right] \exp\left[-\frac{H_\beta^F + H_\beta^m}{kT}\right], \qquad (12)$$

where β stands for either I or V depending on the defect that participates in the diffusion process. From Eq. (12) one can identify Arrhenius like temperature dependency of D with a pre-exponential factor D_0

$$D_0 = f_\beta g_\beta a_0^2 \nu_{\beta 0} \exp\left[\frac{S_\beta^F + S_\beta^m}{k}\right] \qquad (13)$$

and an activation enthalpy H_a

$$H_a = H_\beta^F + H_\beta^m . \qquad (14)$$

Now we have obtained physical interpretation for activation enthalpy (H_a) values and pre-exponential factor (D_0).

Considering the impurity atom diffusion, we have to take into account the interactions between defects and impurity atoms. Interactions are considered to consist of two factors; the Coulomb interaction resulting from ionised impurity atoms and charged defects and second factor resulting from the possible size difference between the impurity atoms and the host crystal atoms introducing local stress in the lattice. The stress is relieved by the presence of point defects: large atoms, compared to the host lattice atoms, attract vacancies and small atoms, compared to host lattice atoms, attract interstitials to fill the extra space in the lattice.

In the case of vacancy- impurity interaction denoted as A-V a binding energy term (E^b_{AV}) can be included in the activation enthalpy and thus yielding a lower activation enthalpy by ΔE [Hu78]

$$H_{AV} = H_V^f - E_{AV}^b + H_V^m + E_{AV}^b - \Delta E = H_V^{SD} - \Delta E\,, \qquad (15)$$

where H_v^{SD} is the activation enthalpy of the self-diffusion. From Eq. (15), it can be seen that the AV-binding decreases the vacancy formation enthalpy and increases the migration enthalpy. The binding energy E^b_{AV} is the potential difference between a vacancy next to an impurity atom and a vacancy far from the impurity atom (equally referred as ΔE_1). According to model for A-V pair diffusion in diamond lattice (like Si and Ge), the ΔE is shown to be $\Delta E = (\Delta E_2 - \Delta E_3)/2 > 0$ [Dun95], where ΔE_2 and ΔE_3 are the binding energies between an impurity atom and a vacancy at the second and the third closest neighbour sites respectively.

In the interstitial assisted diffusion the atomistic movement is more complicated and an analytical expression similar to Eq. (15) is hard to compile. Nevertheless, using similar arguments as those for A-V binding, A-I binding E_{AI}^b is suggested to result in lower activation enthalpies compared to self-diffusion. Indeed, for most impurities in Si and Ge lower activation enthalpies compared to self- diffusion have been observed. The relevant experimental data is overviewed in Sec. 5.

The diffusion coefficient (Eq. (12)) is basically different for diffusion via defects with different charge states. In experiments it is generally difficult to control or identify the charge states of the defects participating in the diffusion. The measured experimental diffusion coefficient values are normally an average for all charge states.

A relevant question concerning diffusion is the effect of mass or the so-called isotope effect. Each element has several isotopes, which are chemically identical, but differ in mass. As we can see from Eq. (12) diffusion is not dependent on the mass explicitly. Assuming the harmonic force response of the attempt frequency $\nu_{\alpha 0}$ (i.e. $\nu_{\alpha 0} \sim m^{-1/2}$), the isotope effect can be formulated as

$$\frac{D_a}{D_b} = \frac{\nu_{a0}}{\nu_{b0}} = \sqrt{\frac{m_b}{m_a}}, \qquad (16)$$

where a and b denote isotopes with different masses. According to Eq. (16) the isotope effect is most pronounced for light elements.

4 Experimental methods for solid-state diffusion

4.1 Conventional techniques

The large amount and variety of diffusion studies and materials have yielded numerous of different experimental methods for measurement of diffusion properties both qualitatively and especially quantitatively [Bor88].

The major principle in all experimental diffusion studies is to know and control the conditions and all parameters, which affect diffusion (see Sec.3.3). First, it is essential to characterise the quality of the diffusion samples. As it was described in Sec. 3.3, the amount of impurities and other imperfections may affect the diffusion parameters under study. Second step is to deposit diffusing element into the sample material. It can be deposited on the sample surface using several techniques [Rot84]. Since the sample surface may be exposed to disturbing chemical reactions, it is better to introduce the diffusing element under the sample surface. For this purpose ion implantation or MBE-grown hetero structures [Fuc95] can be used. The concentration of the diffusing element as well as the initial (after deposition-) conditions for diffusion must be controlled and known. Thirdly, diffusion annealing is usually required for substantial diffusion to occur and the annealing conditions must be well established. This means that accurate temperature measurement and chemically stable conditions are required. Finally the redistribution of the diffusing element must be determined quantitatively after annealing, i.e. depth profiling of diffusing element is required.

The major principle in most diffusion studies is to determine the depth profile of the diffusing element before and after atom redistribution in the solvent matrix. Only a short review of the most frequently applied and some novel methods are presented in the following.

The depth profiling methods can be divided into two categories: direct chemical profiling and indirect profiling. In the case of semiconductors the indirect methods are based on

changes observed in the electrical properties due to the redistribution of the diffusing atoms. The most applied of such techniques is the spreading resistance method [Maz90]. These methods are restricted to atoms, which act as donors or acceptors in semiconductors and the correlation between the diffusing element concentration and donor or acceptor concentration must be made. This assumption is known to fail at the high diffusing element concentration (see for example [Nob94]), as the clustering and precipitation electrically deactivate the diffusing atoms.

Direct methods can be further divided into two categories: non-destructive and destructive methods. Widely applied non-destructive ion beam methods are Rutherford Backscattering Spectrometry (RBS) and Elastic Recoil Detection Analysis (ERDA) both of which are based on the well-known elastic ion scattering [Chu78,]. The problem with these techniques is the lack of sufficient sensitivity due to the low scattering probabilities (i.e. cross sections). The detection limits for RBS or ERDA are typically 10^{18}-10^{20} atoms/cm^3, which are much higher than required for impurity atom diffusion studies in intrinsic semiconductors.

The destructive methods are usually based on consecutive erosion of the sample surface (also called as serial sectioning). The profile construction is made by either detecting the traced element from the eroded material or from the material, which is left on the sample. The serial sectioning can be performed by clapping or grinding, when the profiled depths are of the order of micrometers [Rot84].

The miniaturizing of modern electronic devices necessitates also smaller scales in diffusion research and therefore the so-called micro sectioning is required. In this case the ion beam sputtering can be used for serial sectioning. The best-known sputtering-based profiling method is Secondary Ion Mass Spectrometry (SIMS), which is a widely applied powerful tool for depth profiling and chemical analysis with good sensitivity (down to 10^{17} atoms/cm^3) and excellent depth resolution (few nm). In SIMS the analysis is based on mass resolving of the emitted ions from the eroded sample surface. A problem with SIMS is the complexity of the emission phenomena, as the ion-emission probability is still poorly known. This can make quantitative analysis with SIMS rather troublesome. There are

several attempts to overcome this problem, for example, via post ionization of the emitted neutral atoms [Ben87].

The lack of sensitivity is a general problem in experimental depth profiling especially for semiconductors. To overcome this problem, radiotracers can be used. Radiotracers are non-stable isotopes of the diffusing element, which emit radiation in their decay. Emitted radiation is relatively easy to detect, yielding excellent sensitivity for the diffusing element. The major drawbacks are the expenses and the availability of radioactive material production. Also the number of proper tracer isotopes is rather limited. In the typical experiment employing the radiotracer technique, the tracer is deposited on the sample surface by evaporation or embedding the samples in a liquid or gas in sealed ampoules. After diffusion the samples are serial sectioned usually either by clapping or grinding [Rot84].

One emerging depth profiling technique is Accelerator Mass Spectrometry (AMS) or Accelerator SIMS [McD03], which combines the benefits of SIMS and tracer methods. In this technique sputtering is also used for serial sectioning and the emitted ions are first accelerated and then detected with radiation detectors. The sensitivity of this method is strongly dependent on the traced element, since due to the employed type of the accelerator, the sputtered ions must be usually emitted as negative ions. This probability is not accurately known and it may vary strongly with the sputtering conditions. Typical detection limits obtained for depth profiling with AMS technique are order of 10^{14} atoms/cm^3 [Mit04].

Also in the modified radiotracer technique the benefits of SIMS and tracer method are combined. In this technique the tracers are deposited by implantation minimizing surface effects affecting diffusion. This technique has the same excellent depth resolution (few nm) as SIMS and AMS, but a superior sensitivity over SIMS and even over the AMS technique. Typical detection limits are 10^{11}-10^{13} atoms/cm^3 depending on the tracer (Sec. 4.2.1) and detection system (Sec. 4.2.4). Major drawback is that the technique requires radioactive ion-beams, which are available only in few laboratories in the world. In the following, detailed description of the modified radiotracer technique is presented.

4.2 Diffusion studies by the modified radiotracer technique

The basic principles of the modified radiotracer technique are presented in Fig. 4. The technique includes following steps: (i) the first step is the production and implantation of the radioactive isotopes of the diffusing element, denoted as tracers. (ii) After the implantation the samples are annealed.

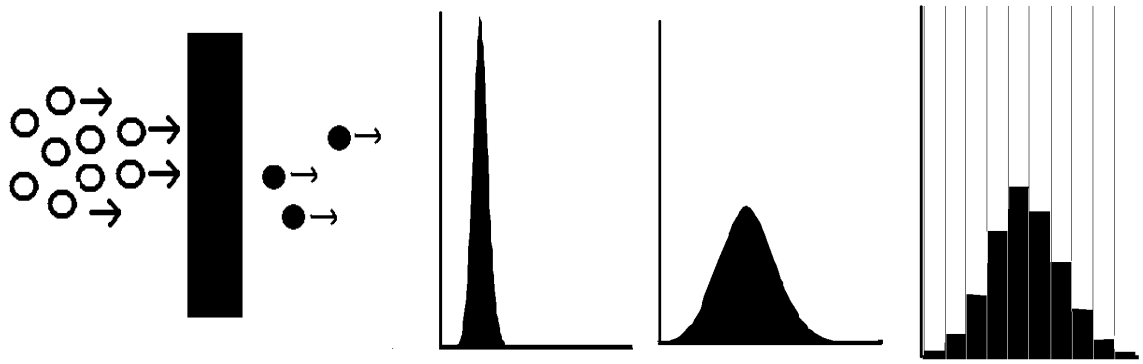

Fig. 4 Experimental steps of the modified radiotracer technique.

(iii) Then the sample is serial sectioned by sputtering followed by activity measurements of the eroded material and the depth profile construction, and (iv) finally the quantitative analysis of the experimental depth profile is performed.

4.2.1 Radiotracer production and deposition

The radiotracer method requires radioactive isotopes of the diffusing element. The mass of the tracer isotope differs from that of stable isotopes existing in the nature. Usually, when diffusion is concerned, the distinction between different isotopes is not made, since the effect of the mass difference can be considered to be negligible in most cases (see Eq. (16)).

The decay of this unstable radiotracer nucleus has to occur in such way that it emits detectable quanta either directly or indirectly. Suitable quanta are alpha particles (α),

electrons (e^-), positrons (e^+), gamma rays (γ), and X-rays. Another requirement for the tracer isotope is the proper half-life (decay probability). The activity of the radiotracers follows the equation

$$A = \frac{\ln 2}{T_{1/2}} N \,, \tag{17}$$

where the $T_{1/2}$ is the half-life of the decaying radio-nuclide [s] and N their number.
The time evolvement of the activity is

$$A = A_0 \exp\left[-\left(\frac{\ln 2}{T_{1/2}} \right) t \right] = \frac{\ln 2}{T_{1/2}} N_0 \exp\left[-\left(\frac{\ln 2}{T_{1/2}} \right) t \right], \tag{18}$$

where the subscript 0 denotes the initial values at the chosen time.

Basically the upper limit of the tracer half-life is set by the patience of the researchers (or available time for the experiments) whereas the lower limit of the half-life is set by the time required for the whole experimental sequence following implantation together with the available deposition activity. The faster the decay of the tracer, the higher sample activity is required. In practice, the isotope successfully used in diffusion studies with the shortest half-life is ^{11}C ($T_{1/2}$= 20.3 min) [Str02, Vos03]. An especially designed experimental set-up for "short- lived" tracers [Vos02] has to be employed in such cases. Typical tracers half-lives vary from tens of minutes (like ^{11}C) to months (like ^{195}Au, $T_{1/2}$= 183 d).

The production rate of the radiotracer has to be sufficiently high and the resulting reaction products must be possible to be ionised and implanted into diffusion samples. The most convenient way is to use the isotope separator on -line (ISOL) technique, where the collection of the reaction products, their ionising, separation and acceleration is performed in sequence and continuously (on-line) with the production of radionuclides. In the present work, the tracers are produced applying this technique at ISOLDE- (ISotope On-Line DEvice) facility [ISOLDE] of the European Organization for Nuclear Research CERN,

Geneva and at IGISOL (Ion-Guide Isotope Separator On-Line)- facility [Dendooven97] in the Accelerator Laboratory of Jyväskylä University (JYFL). Some of the tracer implantations were realised by employing the more conventional method where the radioactive material is produced in a nuclear reactor and is post-ionised followed by the tracer mass separation and implantation. This method was employed at the mass separator of the Institut für Strahlen- und Kernphysik at Bonn University, Germany.

The time required for one sample implantation depends on the ion flux and the activity required for successful depth profiling. The time evolvement of the activity during the implantation follows equation

$$A = I\left\{1 - \exp\left[-\left(\frac{\ln 2}{T_{1/2}}\right)t\right]\right\}, \qquad (19)$$

where I is the implantation flux. According to Eq. (19) the maximum obtainable activity in the sample equals to the implantation flux. The required activity in the sample depends on the half-life, annealing conditions (Sec 4.2.2) and detection efficiency (Sec. 4.2.4). It has to be evaluated and tested for each experiment separately.

Other implantation parameters besides time are energy and implantation area. Implantation energy is usually chosen so that the ion extraction and transport of the tracer atoms are optimised. Typical values are few tens of keV, which are also sufficient for the tracer implantation well below the surface (10 - 50 nm). This is important for setting the well-defined diffusion conditions in annealing (Sec 4.2.2). Higher energies would increase the range of the tracer atoms, but this would also increase the implantation-induced damage in the samples, which would distort the point defect concentrations (Sec. 3.3).

Implantation inevitably induces radiation damage to the crystal. The energy of the implanted ions is transferred by collisions to sample atoms bunching them from their original lattice sites. Most of them are found to return back shortly after the replacement [Nor97], but some damage remains. The effect of this defect excess on diffusion is found to be negligible for

typical fluences employed in radiotracer studies (10^8-10^{11} cm^{-2}) (Articles IV and V). Radiation damage, however, limits the amount of usable sample activity together with possible health hazards caused to the researchers.

4.2.2 Diffusion annealing

Generally diffusion is too slow in room temperature for practical experiments. Therefore it must be enhanced by increasing the sample temperature (see Eq. (4)). This is realized by annealing the tracer-implanted samples at elevated temperatures. As it was described earlier (Sec. 3.3), the concentration of defects, which is a critical factor for diffusion, may be altered by chemical reactions at the sample surface. This means that during annealing all possible chemical reactions at the surface must be either avoided or controlled. In the present work, diffusion properties under thermal equilibrium were studied and thus all chemical reactions are harmful. These can be avoided by annealing the samples in inert gas ambient such as Ar or under high vacuum conditions together with a getter foil, which absorbs possible residual gas atoms (especially oxygen). Although proper precautions have been taken, the surface can experience chemical changes to some extent. These have a negligible effect on diffusion if the altered layer is significantly thinner than the range of the implanted tracers. In this case the distribution of defect excess does not reach the region, where the followed diffusion occurs.

The precise temperature control during the annealing is also essential. This is realized by attaching a thermocouple to the sample. Also the heating up and cooling down periods must be significantly shorter than the annealing time or these transient temperature periods must be taken properly into account [Rot84].

The annealing time and temperature determine the redistribution of the diffusing tracer. The average diffusion displacement (i.e. diffusion length) x_D of the tracer can be calculated by

$$x_D = \sqrt{4Dt}\,, \qquad (20)$$

where D is the diffusion coefficient at the annealing temperature and t is the annealing time. The x_D values set the characteristic distance of the experimental depth profile (Sec 4.2.3) and it has to exceed the depth resolution but not the accessible depth range of the profiling technique. The proper adjustment of x_D requires an initial guess for the D value and it often takes several attempts to find the proper annealing parameters for successful depth profiling.

For the determination of the activation enthalpy H_a and the pre-exponential factor D_o (Eq. 4) the covered temperature range is an essential feature. It is the most determining parameter for the accuracy of H_a and D_o (Sec. 4.2.5). Wider the temperature range is the more reliable values for H_a and D_o are obtained.

4.2.3 Serial sectioning by sputtering

The principle of serial sectioning by ion beam sputtering has been widely applied and studied especially for SIMS. In the radiotracer method sputtering has the same requirements as in SIMS [article V], but less instrumentation is involved [Ben87]. The basic requirements are controlled and spatially homogenous eroding of the sample and collection of the eroded material for further analysis. The homogenously eroded area must be larger than the implantation area, so that the distortion of the determined profile due the edges of the formed crater can be avoided.

The eroding speed sets the practical range of the depth profiles, since due to the decaying tracers depth-profiling time is often limited. With intensive ion beams, typical eroding speeds are few tens of nm/min; enough that profiling can be extended to few microns in depth. The eroding speed depends on ion flux and sputtering yield. Sputtering yield in turn depends on the ion energy and angle of incidence with respect to the sample surface. For a fixed energy, the obtainable flux is a feature of the sputtering device that can be adjusted in several ways [Article V]. Sputtering energy and angle are easily adjustable parameters and sputtering yield can further be affected by changing the ions.

The sputtering yield and also the maximum flux from the ion-source usually increase as the energy is increased up to few tens of keV [Roo81]. The increasing of the sputtering energy results in deeper and larger collision cascades in the material. This in turn decreases the depth resolution in serial sectioning as the particles are emitted from a larger depth range [Ben87]. In practice the sputtering energy is kept low (0.5-5 keV) to guarantee good depth resolution and therefore the eroding speed is maximized by the other parameters. The sputtering yield has been found to have a maximum value, when the angle between the incoming beam direction and the sample surface normal is 60-70^{o} [Roo81]. Sputtering at a glancing angle also improves the depth resolution, as then the collision cascades form closer to the sample surface. Also, the heavier the sputtering ions are, the denser and shallower collision cascades are formed resulting in improved depth resolution [Ben87].

Besides the range and density of the collision cascades, the depth resolution is also affected by the smoothness of the sputtered surface and grain boundaries. For example in case of Si, it has been found that sputtering with O and N ions result in smoother sample surfaces than obtained with noble gasses [Ber81].

In this study all samples are single crystalline and they become amorphous during sputtering (since both Si and Ge do [Ber81]), so the major parameter affecting the depth resolution is the sputtering energy.

The eroded material must be collected for further analysis and this is realized by collecting the sputtered material to a Mylar foil placed as close as possible to the sputtered sample. The collection efficiency has been optimised by using a large collection area and placing the foil adjacent to sample surface normal corresponding to the most probable emission direction [Ber91]. When one layer has been eroded, another collection foil segment is moved in the collection position and the previous foil segment is wrapped on a roll like a film in a camera. In this way up to 40 foil segments can be collected each corresponding certain depth slice of the sample. As previously reported [Mun83] no cross-contamination

between the foil segments has been observed even if the segments are in physical contact with each other.

4.2.4 Activity measurement and profile construction

The last experimental step in the depth profiling is the activity measurement of the collection foils. Since the amount of the tracer is directly proportional to the activity in each foil, the profile construction is a rather straightforward procedure.

The thickness d_i of each depth slice i (corresponding measurement of one foil segment) is

$$d_i = \frac{\Phi_i}{\Phi_{tot}} d_{tot}, \qquad (21)$$

where Φ_i and Φ_{tot} are the sputtering ion flux exposed to the sample during the collection of slice i and the total exposed flux to the sectioned sample respectively. d_{tot} is the depth of the sputtered crater, which is measured after sputtering by a profilometer.

The relative concentration of the tracer in each slice equals to the activity of the corresponding foil segment corrected with decay of the tracer and normalized with the thickness of the slice. The decay correction is made using Eq. (18) The half-lives of the tracers are in this study much longer than the measurement time of the individual foil segment, so that change in activity during single activity measurement can be neglected.

For depth profiling it is sufficient enough to determine the relative concentration change as function of the depth. In order to do that the measurement conditions and the geometry

must be kept constant during the measurement of the depth profile. The major error source in the activity measurements is the variation in the positioning of the collection foil segments in front of the detector. This can be avoided by using a detector with large solid angle [Article I] and defining properly the foil collection area and the active area of the detector. Using a large solid angle detector in the measurements also guarantees the high efficiency for the tracer detection. Although the absolute detection efficiency does not affect the shape of the profile it is an important feature in the profiling. Efficient detection decreases the required amount of the implanted ions or/and reduces the time needed to obtain sufficient statistics in the activity measurements.

Background subtraction is also a very important factor to be taken into account. The concentration profiles are usually measured as deep as possible where the measured activities are close to the background level. Then the information on the relative activities between the foils is not any more possible to obtain.

The detector type for the activity measurement is chosen depending on the emitted radiation of the tracer or its daughter nuclei. For detection of alpha particles, electrons and positrons a Si- based semiconductor detector systems like the detector described in Article I or strip detectors can be used. For the γ- and x-rays radiation cooled large volume Ge-detectors and scintillation detectors are commonly employed.

4.2.5 Analysis of the experimental depth profile

Once the experimental profile is obtained, the quantitative analysis is made in order to obtain the diffusion coefficient D (Eq. (1)) at the given temperature. The initial conditions for the diffusion are determined by measuring the depth profile of a non-annealed implanted sample (i.e. “as- implanted” profile). A Gaussian function

$$C(x,t=0) = C_0 \exp\left[-\frac{(x-x_c)^2}{2w^2}\right] \tag{22}$$

is then fitted to this profile. C_0 is the total concentration of the tracer in the sample, x_c is the peak position (or middle point) of the profile and w is the standard deviation (broadness) of the profile.

To the profiles obtained for the annealed samples, the equation

$$C(x,t) = \frac{C_0}{2\sqrt{1+\frac{2Dt}{w^2}}}\left[\begin{array}{l} erfc\left(-\frac{\frac{x_c}{2w^2}+\frac{x}{4Dt}}{\sqrt{\frac{1}{2w^2}+\frac{1}{4Dt}}}\right)\exp\left(\frac{(x-x_c)^2}{2w^2+4Dt}\right)+ \\ k\cdot erfc\left(-\frac{\frac{x_c}{2w^2}-\frac{x}{4Dt}}{\sqrt{\frac{1}{2w^2}+\frac{1}{4Dt}}}\right)\exp\left(\frac{(x+x_c)^2}{2w^2+4Dt}\right) \end{array}\right] \tag{23}$$

is fitted, where the parameter k represents the different boundary conditions at the sample surface (x=0). This parameter varies between k = -1 corresponding to a surface acting as a perfect sink

$$C(x=0,t)=0 \tag{24}$$

and k = +1 corresponding to an ideally reflecting surface

$$\left.\frac{\partial C(x,t)}{\partial x}\right|_{x=0} = 0\,. \tag{25}$$

Eq. (23) reduces with t = 0 and k = 0 to Gaussian profile of Eq. (22), fulfilling the initial conditions. For a given depth profile, the solution given in Eq. (23) is fitted so that x_c and w have fixed values obtained from a Gaussian fit to the as-implanted profile (Fig. 5a) and k, C_0

and x_D are free parameters. As a result from such fit x_D is extracted and the D value is calculated by using Eq. (20) (Fig.5b).

After the determination of D values at several different temperatures, the diffusion parameters H_a and $D_{0,}$, can be determined (see Eq.(4)). This requires that a straight line fit be obtained to the D values plotted as function of T^{-1} on semi-logarithmic scale (Articles III-

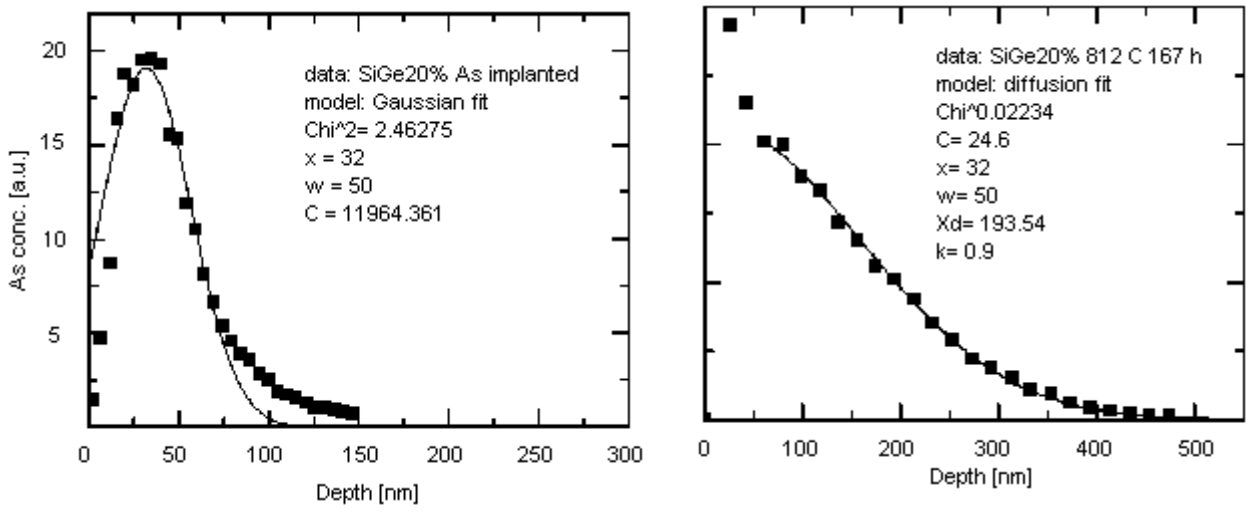

Fig. 5 a) Example of the fitting of a Gaussian curve (Eq. (22)) to the as implanted profile. Parameters x and w are extracted from the fit. b) Fitting of the solution of the diffusion equation. (Eq. (23)) to the profile for an annealed sample. The mean diffusion length x_d [nm] is extracted from the fit.

As it can be also noted from Fig. 5, that the as implanted profile is not exactly of Gaussian shape. For example, the Pearson distribution describes the implantation profiles precisely [Bow92]. After examining the same profiles employed both Gaussian and Pearson IV functions to describe the initial diffusion conditions, we found no systematic or significant difference in the obtained D values. Using the Gaussian function the diffusion equation can be solved analytically (Eq. (23)) yielding straightforward and easy analysis of the profiles. In general, when the diffusion profiles are significantly broader than the initial profile (x_D >w), the D values are not very sensitive to the initial profile shape in the fitting process.

5 Diffusion in SiGe

In this chapter the present day knowledge on diffusion in SiGe is presented. Although strained and extrinsic SiGe is technologically more important, this chapter is focused on relaxed, intrinsic SiGe. Especially the dependency of the diffusion rate and mechanism on the SiGe composition is reviewed.

First, the diffusion in its components Si and Ge is surveyed emphasizing cases, which are comparable to those studied in SiGe alloys recently.

5.1 Self- and impurity diffusion in Si and Ge

5.1.1 Si self-diffusion

The debate over the self-diffusion properties in Si has a long history. There are numerous studies giving activation enthalpies between 4-5 eV with suggestions that the interstitials, vacancies, both or neither [Pan89], are responsible for the diffusion migration of self-atoms [Fra84].

The concentration of vacancies (C_v^{eq}) from analysis of diffusion data of metal atoms in silicon can be described according to Bracht [Bra95] by

$$C_v^{eq} = 2.8*\exp[-2.0\ eV/kT] \qquad (24)$$

and accordingly interstitial concentration (C_I^{eq}) by

$$C_I^{eq} = 58*\exp[-3.18eV/kT]. \qquad (25)$$

This means that the concentration of vacancies is two orders of magnitude larger than the concentration of interstitials (T= 870-1208^{o}C). This observation is also supported by several other experimental studies [Zim92, Bro87, and Boi90], although there are large discrepancies in the C_I^{eq} values, depending on method used.

The diffusivity of vacancies and interstitials can be described by [Bra95]

$$D_V = 3.0*10^{-6}\exp[1.8eV/kT]\ m^2/s \quad (26)$$

and

$$D_I = 5.1*10^{-3}\exp[1.77eV/kT]\ m^2/s. \quad (27)$$

This in turn means that the diffusion of interstitials is about two orders of magnitude faster than of vacancies. As a result of the values in Eq. (24-27) the self-diffusion (Eq. (12)) via both defects are comparable (Fig. 6). From this follows that

$$D_V^{SD} = 4.2*10^{-6}\exp[-3.8eV/kT]\ m^2/s \quad (28)$$

and

$$D_I^{SD} = 1.2*10^{-1}\exp[-4.95eV/kT]\ m^2/s, \quad (29)$$

when f_v= 0.5 [Gös80], f_I=0.73 [Kom58]. The results suggest that at high temperatures (T > 1050^{o}C) the interstitialcy mechanism dominates and lower temperatures (T < 1050^{o}C) the vacancy mechanism dominates self-diffusion in Si. The Zn out-diffusion studies by Giese [Gie00] yielded

$$D_V^{SD} = 1.1*10^{-4}\exp[-4.24eV/kT]\ m^2/s. \quad (30)$$

Similar results have been also obtained from other metal in-diffusion [Tan85, Mor88] and out-diffusion (Ni) [Yos67] studies.

The recent results for self-diffusion in Si give [Bra98]

$$D^{SD} = 5.3*10^{-2}\exp[-4.75eV/kT]\ m^2/s, \quad (31)$$

which is further confirmed by Ural [Ura99]. According to Fig. 6 these results are in accordance with the results obtained from metal diffusion studies (Eq. (28) and Eq. (29)). The results of Giese (Eq. (30)) suggest that crossover of the self-diffusivity via interstitials and vacancies occurs already at T=890^{o}C, which is supported also by Bracht self-diffusion results [Bra98].

The major difference between the two consistent results [Bra98, Ura99] is the interpretation of the underlying diffusion mechanisms. Bracht et al. deduce that the self-diffusion is dominated by interstitials, since to the obtained experimental data a single Arrhenius line can be fitted. Ural et al. in turn employing studies under point defect injection (oxidation and nitridation, see Sec 3.3) have found that the properties of the interstitials and vacancies follow [Ura99]

$$D_I^{SD} = 1.5*10^{-2}\exp[-4.68/kT] \quad (32)$$

and

$$D_v^{SD} = 6.4*10^{-2}\exp[-4.86/kT], \quad (33)$$

and therefore the contribution of both defects to the diffusion is more or less equal and temperature independent.

In conclusion, there is no controversy in the diffusion parameters D_0 and H_a, but there is still no consensus on the microscopic picture behind these values. This is mainly due to the differing results obtained from metal diffusion studies and point defect injection studies. The major problem still is that the C_I^{eq} and C_V^{eq} values are not yet been able determined accurately enough for closing the debate.

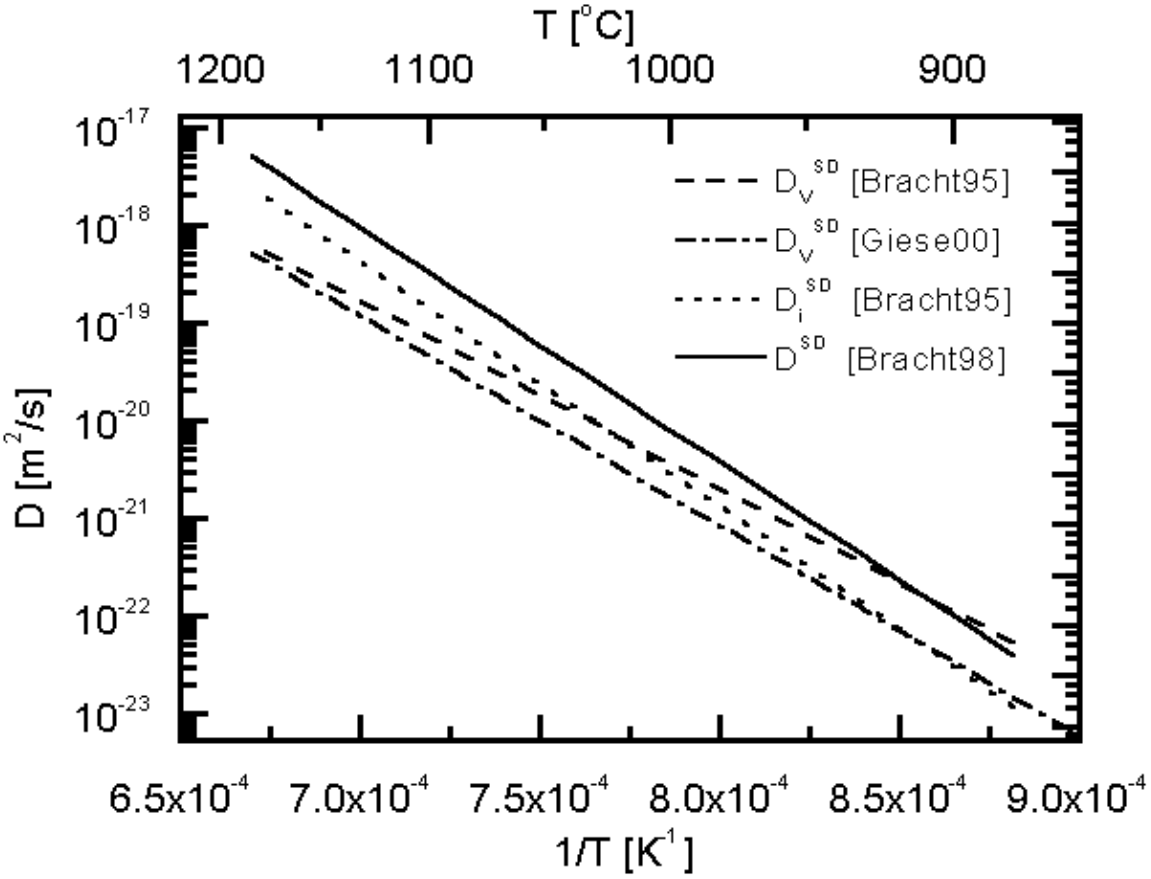

Fig. 6 Self-diffusion via interstitials and vacancies as determined from metal data [Bra95, Gie00] and self-diffusion data in Si by Bracht [Bra98].

Calculations seem to qualitatively support the model provided by metal diffusion studies, i.e. that interstitials dominate self-diffusion at high temperatures and vacancies dominate it at low temperatures [Tan97, Jää01]. Although the calculations provide comparable self-diffusion coefficients with experiments, they predict higher concentration and slower mobility for interstitials over vacancies, which is opposing with the experimental results (Eq. (26-29)).

5.1.2 Impurity diffusion in Si

Impurity diffusion in Si has been studied for more than 30 elements [Sch02]. Elements, which dissolve to interstitials sites like the small atoms H, Li, Na, K and the larger Mn, Cr, Fe, Ni, Cu atoms, diffuse fast via the direct interstitial mechanism (H_a= 0.1-1.2 eV). Most

impurities dissolve to substitutional sites meaning that the diffusion requires participation of defects. This leads to a much slower diffusion with H_a = 2.5-5 eV. There are also elements, which may dissolve either to interstitial or substitutional sites and the diffusion proceeds via kick-out and dissociative mechanisms. This has been found to be the case for C, Zn, Ag, Pt and Au. The diffusion rate of these atoms is intermediate compared to the two previous cases.

The simplest cases for the impurity diffusion are the elements from group IV of the periodic table, since there are no electrical effects due the impurities. As mentioned earlier, carbon diffuses [Gös86] via kick-out mechanism. From studies employing the point defect injection, the interstitial fraction value for Si self- diffusion has been found to be f_I = 0.5-0.6 [Ura99] and for other group IV elements f_I = 0.4-0.5 for Ge [Fah89] and f_I = 0 for Sn [Kri97]. The interstitial fraction seems to decrease with increasing size of the diffusing element. This is considered to result from elastic effects (Sec. 3.4) favouring vacancies over interstitials as the size of the impurity atom increases.

Typical dopant atoms such as P and B diffuse via interstitials and Sb via vacancies. Arsenic has been found to diffuse similar to self-diffusion via both interstitials and vacancies. The diffusion parameters for typical dopant atoms are compiled to Table I together with results for some group IV elements. The results show that group IV elements have comparable activation enthalpy values with those of self-diffusion whereas group III and V elements diffuse faster due to the lower H_a values. Also interstitial mediated diffusion is generally faster than vacancy mediated diffusion.

The reasoning for these experimental findings described above is based on the model by Seeger and Chick [See68]. In their model interstitials act as donors under p-type conditions resulting in interstitial mediated diffusion for the group III elements due to Coulomb attraction. Under n-type conditions interstitials are acceptors like vacancies, which cause attraction of group V elements by both defects. In this case the diffusion mechanism (similar to group IV elements) is determined by the elastic interaction (size) between the impurities and defects (see Table I). In addition the Coulomb attraction between impurities and defects

is considered to be stronger than the elastic effects. This explains the lower H_a values for group III and V impurities than obtained for group IV impurities (Table I). Although the model oversimplifies the structure of the defects [see for example Wat81], it provides qualitative explanation to the impurity diffusion behaviour of groups III-V elements as well as to doping dependence of Si and Ge self-diffusion. Namely, both n- and p- type doping enhances the self-diffusion of Si whereas in Ge self-diffusion via vacancies (Sec. 5.1.3) is enhanced by n- doping and retarded by p- doping.

Table I Self- and impurity atom diffusion parameters for Si.

diffusing atom	H_a [eV]	D_0 [m^2/s]	interstitial fraction f_I (temperature range)	references
Si	4.75	0.053	0.3-0.71 (T=1000-1100 ^oC)	[Bra98, Ura99]
Ge	4.7	0.25	0.3-0.4 (T= 1050^oC)	[McV73,Fah89]
Sn	4.8	0.14	~ 0 (T=1000 ^oC)	[Kri97]
B	2.85	0.0021	0.84-1 (T=1000-1100 ^oC)	[Gho71a, Ural99]
P	3.30	0.074	0.84-1 (T=1000-1100 ^oC)	[Gho71a, Ural99]
As	3.44	0.065	0.15-0.54 (T=1000-1100 ^oC)	[Gho71b, Ural99]
Sb	3.65	0.21	0-0.016 (T=1000-1100 ^oC)	[Gho71a, Ural99]

5.1.3 Self- and impurity diffusion in Ge

Self- and impurity diffusion in Ge is less extensively studied and the results are less controversial than in the case of Si. It is generally accepted that both self- and impurity diffusion in Ge proceed via vacancies. The experimental self-diffusion results are in fairly good agreement with each other [Fra84, also compiled in Article IV] yielding

$$D^{SD} = 0.02 * \exp[3.1\text{eV}/kT] \ \text{m}^2/\text{s}. \qquad (31)$$

The self-diffusion of Ge is several orders of magnitude faster than of Si [see for example Article III]. The pressure dependence of Ge self-diffusion [Wer85] and the dissociative mechanism prevailing for the diffusion of metals such as Cu [Sto84], Zn [Alm91], Ag and Au [Bra91, Str01] are convincing evidence on vacancy concentration dominance over interstitial concentration.

Impurity atoms are considered also to diffuse via vacancies, as they are dominant point defects in Ge. The diffusion results for group IV impurities and typical dopant atoms are compiled to Table II. The results show that impurities with the same valence as Ge, that is Si and Sn, diffuse accordingly to their size compared to the size of Ge, i.e. Si slower and Sn faster. This feature can be explained by the elastic interaction (Sec 3.3). The group III impurity B diffuses slower and group V impurities faster than for self-diffusion. This is in agreement with the model by Seeger and Chik presented in the previous chapter. Vacancies are acceptor and thus they are attracted by group V elements and repelled by group III elements due to the Coulomb interaction.

Table II Self- and impurity atom diffusion parameters for Ge.

diffusing atom	H_a [eV]	D_0 [m^2/s]	references
Ge	3.14	0.0081	[Article I]
Si	3.19	0.0041	[Article II]
Sn	3.26	0.084	[Fri95]
B	4.5	960	[Mee67]
P	3.1	0.033	[Mat78]
As	2.42	0.00058	[Article IV]
Sb	2.57	0.00065	[Sha90]

There are, however, some experimental results providing exceptions to the coherent Ge diffusion data. Mitha et al. [Mit96] observed that pressure dependence of As diffusion in Ge cannot be explained only by diffusion via vacancies, but also the participation of interstitials must be considered. Uppal et al. [Upp01] in turn measured the B diffusion in Ge by SIMS obtaining several orders of magnitude smaller values than it was obtained in considerably older studies by resistance measurements.

5.2 Self- and impurity diffusion in SiGe

Clearly the diffusion properties of self- and impurity atom diffusion in Si and Ge are different. In this light it is expected that the diffusion properties of $Si_{1-x}Ge_x$ will experience changes as a function of composition x. At which compositions and how these changes happen, have become the major interest recently. This chapter focuses on this matter, although SiGe has shown to be an excellent playground also for studying defect complexes [Mes03] and strain effects to diffusion [for example Cow94, Kuo95a, Zan03]. Unless otherwise noted, by SiGe is meant intrinsic relaxed single crystalline silicon germanium.

5.2.1 SiGe self-diffusion

The first survey on self-diffusion in SiGe was performed by McVay and DuCharme [McV74], where the H_a and D_0 values for ^{71}Ge in polycrystalline $Si_{1-x}Ge_x$ throughout the composition range x were determined. The reported diffusion rates are significantly higher than the more recently reported values for relaxed single crystalline SiGe by Zangenberg [Zan01] (Table III). Fast grain boundary diffusion is most probable reason for this discrepancy in the D values. The results of both studies, however, indicate that there is a change of the Si-like diffusion mechanism (vacancy and interstitial mediated) to the Ge-like mechanism (vacancy dominated) in the composition region x = 0.2 - 0.4. Both studies give also qualitatively similar results for the H_a values as a function of x: when the x increases the H_a values decrease until they equal H_a value of Ge (3.1 eV). Equal H_a values are found to exist already at compositions x = 0.3 in Ref [McV74] and x = 0.5 in Ref [Zan01]. Comparing the compositional dependencies of the H_a values for self-diffusion to the corresponding values for impurity diffusion in SiGe (Sec. 5.2.2), it can bee seen that they are in contradiction with the model for impurity diffusion via vacancies (model of Hu in Sec. 3.4). Zangenberg et al. note this fact but give no explanation to it in their work.

The most resent study on Ge self-diffusion in SiGe [Article III] confirms the change of the diffusion mechanism to that of Ge at the composition x = 0.35. These results show, though, qualitatively differing behaviour of H_a when the diffusion is fully vacancy controlled (x >

0.35). The activation enthalpy H_a seems to decrease smoothly from ~ 4.0 eV to 3.1 eV as Ge composition is approached (Table III). This is in agreement with the impurity diffusion results (Sec. 5.2), when model of Hu´s is concerned. Also theoretical calculations support qualitatively the compositional evolvement of H_a observed in Article III. The calculations by Venezuela [Ven02] predict that the vacancy formation enthalpy decreases as the number of Ge atoms in the closest neighbourhood of the vacancy increases. This means that the higher the value of x is, the lower the activation enthalpy is due to the lower vacancy formation enthalpy (Eq. (12) in Sec 3.4). Qualitatively similar results have been provided also by the other theoretical work of Ramanarayanan [Ram03].

The aim of Article IV was to check the widely acknowledged argument that Si and Ge behave so alike (like in Ref. McV73), that they also diffuse identically. Based on this Ge has been used to simulate the diffusion of Si. An apparent need for this assumption has been the difficulty of measuring Si diffusion. The present results show that indeed in $Si_{0.2}Ge_{0.8}$ the diffusion of ^{31}Si and ^{71}Ge are close to each other, but not exactly same. Si self-diffusion has a slightly higher activation enthalpy (~0.1 eV) resulting in slightly slower diffusion. The calculations by Venezuela [Ven02] also support these results, as there are somewhat less (on average) vacancies in the vicinity of a diffusing Si atom than of a Ge atom due to the higher vacancy formation enthalpy.

It should still be explained why there are qualitative differences between the experimental in H_a values of Zangenberg and our work. The consideration only of H_a values is somewhat misleading, since the diffusion coefficients also include the effect of D_0, which is too often omitted in the discussions [Gil98], since both the exact values and the physics behind them is more uncertain. By simply comparing the diffusion coefficients at given temperatures obtained in both works [Article V], it can be noted that x- dependencies do not differ significantly. This implies that the qualitative differences in H_a are more virtual than real. When a fit to the same data gives a smaller H_a value it is compensated in the D_0 value (Eq. 4). Indeed in the H_a values reported by Zangenberg, there is a jump down in the H_a values from H_a = 3.7 eV (x = 0.4) to H_a = 3.2 eV (x = 0.5) together with a jump in the D_0 values more than one decade (from $4.2*10^{-4}$ to $1.1*10^{-5}$ m^2/s).

Table III $Si_{1-x}Ge_x$ self-diffusion parameters at various compositions.

Ge[Zan01]			Ge [Article III]		
x	H_a [eV]	$D_0[m^2/s]$	x	H_a [eV]	$D_0[m^2/s]$
0	4.65	$3.1*10^{-2}$	0	4.88	$2.1*10^{-1}$
0.1	4.66	$8.7*10^{-2}$	0.04	4.83	$1.7*10^{-1}$
0.2	4.00	$6.6*10^{-4}$	0.10	4.69	$9.8*10^{-2}$
0.3	3.82	$4.7*10^{-4}$	0.17	4.55	$4.5*10^{-2}$
0.4	3.72	$4.2*10^{-4}$	0.25	4.34	$1.2*10^{-2}$
0.5	3.23	$1.1*10^{-5}$	0.35	4.18	$5.7*10^{-3}$
			0.43	4.04	$5.0*10^{-3}$
			0.50	3.93	$5.1*10^{-3}$
			0.65	3.73	$9.5*10^{-3}$
			0.80	3.48	$8.1*10^{-3}$
			0.85	3.42	$9.8*10^{-3}$
			0.90	3.32	$8.3*10^{-3}$
			0.95	3.31	$2.1*10^{-2}$
			1	3.14	$8.1*10^{-3}$

5.2.2 Impurity diffusion in SiGe

The first systematic surveys on impurity diffusion properties in SiGe at various compositions were performed for Sn [Kri94] and Sb [Nyl96], which were both found to be vacancy diffusers within investigated composition range as it was expected (Sec. 5.1). The compositional dependence of diffusion rate and activation enthalpy show similar decreasing trends with increasing x, although as in pure Si for Sn the activation enthalpy values are anomalously large. The energy barrier for changes in Sn-V pair configuration is suggested to be reason for this [Kri97]. The Sb results are in excellent agreement with Hu´s model, when the resent self-diffusion results [Article III] are taken as a reference. Sb seems to have ~0.5 eV lower activation enthalpies than found for vacancy dominated self-diffusion within

the composition range of $0.35 \leq x \leq 1$. This is in accordance with the calculations for pair diffusion (E-centre) in Si [Pan97, Bun00], indicating that also in SiGe Sb diffuses as a Sb-V pair. Definite conclusions cannot be made, since the properties of vacancies in Si and Ge are found to be different [Faz00], and therefore the vacancy-impurity interaction may change in SiGe as function of composition.

The only impurity diffusion study throughout the whole composition range has been performed for As [Article V]. The compositional dependence of As diffusion resembles that of Sb [Nyl96]. A closer comparison to Sb and self-diffusion results [Article III] reveals, that As diffusion proceeds via both I- and V related mechanisms up to $x = 0.35$ and then changes to a fully vacancy controlled mechanism as it is case of Ge self-diffusion [Article III].

Table IV Diffusion parameters of vacancy diffusers (including As) in $Si_{1-x}Ge_x$ for various compositions.

Sn			Sb			As		
x	H_a [eV]	$D_0[m^2/s]$	x	H_a [eV]	$D_0[m^2/s]$	x	H_a [eV]	$D_0[m^2/s]$
0	4.91	$5*10^{-1}$	0	4.08	$2*10^{-3}$	0	3.81	$4.3*10^{-4}$
0.21	4.61	$8*10^{-1}$	0.1	4.07	$4*10^{-3}$	0.2	3.83	$3*10^{-3}$
0.53	3.88	$8*10^{-2}$	0.2	4.07	$1.3*10^{-2}$	0.35	3.68	$2.3*10^{-3}$
1	3.05	$1.5*10^{-2}$	0.3	3.89	$8*10^{-3}$	0.5	3.47	$1.8*10^{-3}$
			0.5	3.63	$4.2*10^{-2}$	0.65	3.16	$1.6*10^{-3}$
						0.8	2.97	$1.1*10^{-3}$
						1	2.42	$5.8*10^{-4}$

A more dramatic change in the diffusion mechanism is expected for impurities, which are fully interstitial mediated diffusers in Si, and still are expected to diffuse via vacancies in Ge [Sec. 5.1]. Of such impurities Zangenberg has studied the B and P diffusion in SiGe and the results are compiled to Table V. These results show considerable low activation enthalpies

for B and P diffusion in Si compared to other literature data (Table I), but once again they are compensated by the larger D_0 values giving comparable D values. Major reason for this is the relatively limited temperature range (~ 100 ^oC) studied yielding a large deviation in the H_a values (Sec. 4.2.2) although the diffusivity seems to be more or less constant over the studied composition range (Fig. 7). The work of Eguchi [Egu02] confirms the values for P and As diffusion in $Si_{0.8}Ge_{0.2}$.

Table V Diffusion parameters of B and P in $Si_{1-x}Ge_x$ for various compositions.

B			P		
x	H_a [eV]	$D_0[m^2/s]$	x	H_a [eV]	$D_0[m^2/s]$
0	2.68	$3.4*10^{-8}$	0	2.80	$2.0*10^{-7}$
0.01	3.13	$3.4*10^{-6}$	0.07	3.24	$1.8*10^{-5}$
0.12	3.30	$2.4*10^{-5}$	0.12	3.11	$1.1*10^{-5}$
0.24	3.18	$5.7*10^{-6}$	0.24	4.01	$1.7*10^{-1}$
			0.40	3.83	$1.7*10^{-2}$

To get an overview of the diffusion in SiGe all available data is compiled to Fig. 7, where the compositional dependency of D is presented at T= 900^oC. There are three different distinguishable groups of atoms and in Fig. 7 the solid lines represent each group.

The first group corresponds to elements diffusing fully via vacancies throughout the full composition range. For these elements (Sb and Sn) the diffusivity seems to enhance almost linearly with the composition x. This compositional dependence seems to correlate with the melting temperature of SiGe [Stö39], which is the basis for the semi-empirical model by Pakfar [Pak02] that predicts the $D(Si_{1-x}Ge_x)/D(Si)$ ratio as a function of composition x. The melting temperature correlation is supported also the fact that vacancy mediated diffusion is found to follow the Meyer-Nedel rule [Mey36, Kha94] when the change in the melting temperature is included [Zan03b].

The second group includes self- and As atoms. Their diffusivity seems to accelerate more modestly with increasing x at the lower x region compared to vacancy diffusion, and accordingly at the region x > 0.35 indicating the dominance of the vacancy mechanism at this composition range.

The last group includes elements whose diffusion mechanism is interstitial-dominated in Si. Unfortunately systematic studies of these diffusers in the full composition range have not been performed yet. In Fig. 7, the results for B have been compiled from three different studies, where available values for large x are only single D values at T=900°C [Upp03]. There is an obvious lack of experimental data for drawing any definite conclusions, but the qualitative diffusion behaviour of this group compared with the other groups is clear. It seems that the compositional dependency of diffusivity is weak or negligible at least up to the composition of x = 0.4. For B a more modest enhancement can be expected due the

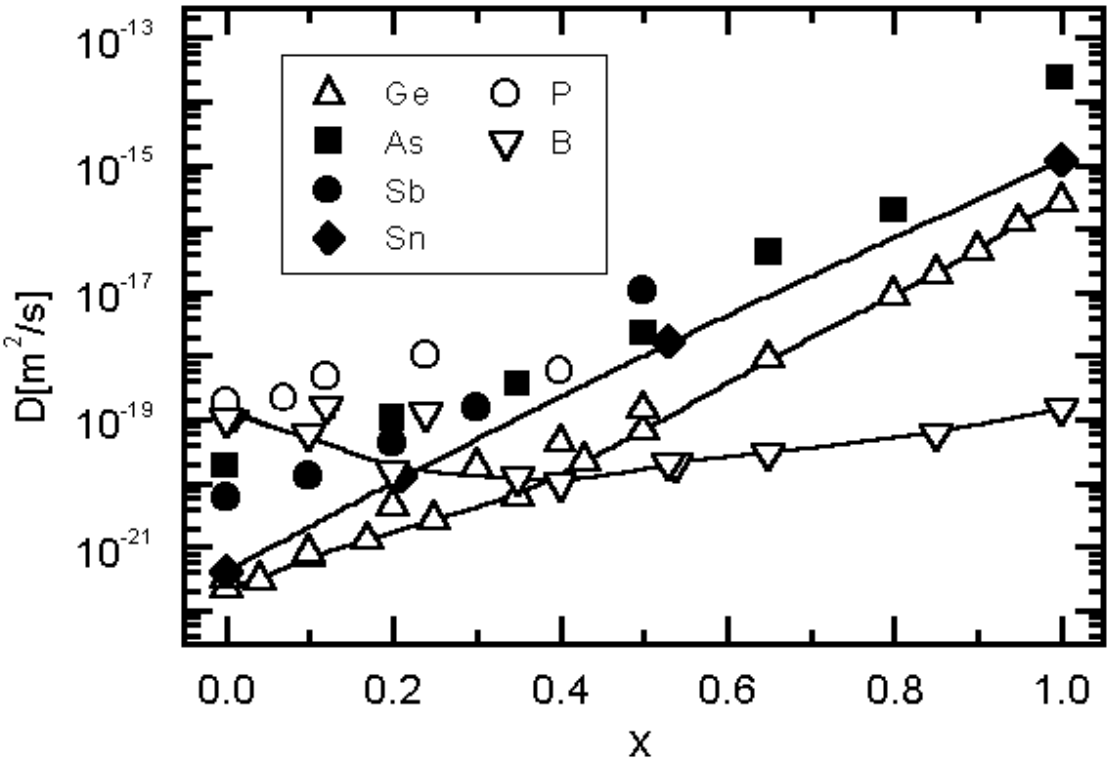

Fig. 7 Self- and impurity diffusion rates as a function of x at 900°C for $Si_{1-x}Ge_x$. The solid lines show the tendencies for self- V- and I mediated diffusion. Data taken from [Article III] and [Zan00] for self-diffusion, [Article V] for As, [Nyl96] for Sb, [Kri94] for Sn, [Kuo95b], [Zan03] and [Upp03] for B, and [Zan03] for P.

composition than for self-diffusion, since B diffusion in Si is faster and in Ge slower than of self-diffusion, but the difference at the Ge rich end is unexpectedly high. If the results of Uppal at higher Ge concentrations are correct, the old data for B and the underlying diffusion mechanism for impurity diffusion in pure Ge must be reconsidered.

The obvious question, what happens to the diffusion mechanism of elements that are I-diffusers in Si as SiGe composition changes towards Ge, is clearly unanswered. The response of B diffusion to strain is found to be similar to self-diffusion up to composition x=0.24 [Zan00, Zan03], i.e. enhancement under tensile strain and retardation under compressive strain. This indicates that up to this composition the diffusion is at least partly interstitial mediated. There are also no theoretical studies on interstitial diffusion in SiGe such as the ones for vacancy diffusion [Ven02, Ram03] lighting up the answers.

Studies on the diffusion behaviour under I- and V-injections could provide useful information. Unfortunately, the only work on this subject, which was found in the literature, is the one by Bonar [Bon01], where the B and Sb diffusion was confirmed to proceed in $Si_{0.9}Ge_{0.1}$ via I and V, respectively.

There is also one study of Au diffusion in SiGe within the composition range $0 \leq x \leq 0.24$ [Fis99]. Although there is a large scatter in the experimental data, this work indicates that in this composition range Au diffuses via kick-out reaction (Sec. 3.2) whereas in Ge Au have been found to diffuse via the dissociative mechanism [Str01]. This only confirms that in SiGe there is a significant interstitial contribution to the self-diffusion at the Si rich end of the composition ($x \leq 0.24$).

Clearly much more experimental data on impurity diffusion in SiGe is needed especially for elements from the third group either to confirm or overrule the picture given in Fig 7. In the light of Uppal´s results it is possible that for B there is no change in diffusion mechanism at all. This would mean a revision of the present picture of impurity diffusion in Ge.

Summary

In this thesis the self-diffusion of Ge and As diffusion in relaxed $Si_{1-x}Ge_x$ were investigated. The activation enthalpies and pre-exponential factors were experimentally determined within the full composition range $0 \leq x \leq 1$. By comparing the observed compositional trends of As and Ge diffusion with the literature data for SiGe, Si and Ge, the change in the diffusion mechanism at x=0.35 was revealed for both elements. This change occurs from both interstitial and vacancy mediated diffusion (x<0.35) to fully vacancy-controlled diffusion ($x \geq 0.35$). The diffusion rate was found to increase as a function of SiGe germanium concentration

A direct comparison of Si and Ge self-diffusion properties was performed at composition x=0.8. These results partly confirm the earlier assumptions of the similarity of Si and Ge atoms as diffusers. On the other hand, according to calculations, the small difference observed in Si and Ge diffusivities confirm that in SiGe-lattice there is a difference in the vacancy formation enthalpy in the neighbourhoods of Si and Ge atoms. This also explains observed self- and As diffusion enhancement in $x \geq 0.35$ composition region.

All experimental results were obtained by the modified radiotracer technique, which offers a unique sensitivity for diffusion studies. The large part of the experimental work of this thesis includes development of instrumentation needed in this technique and its establishment at the Accelerator laboratory of Jyväskylä University.

References

[Abr75] M.S. Abrahams, C.J. Buiocchi and G.H. Olsen, J. Appl. Phys. **46**, 4259 (1975).

[Ahl98] T. Ahlgren, *Diffusion of Impurities in Compound Semiconductors and Diamond-like carbon films*, Ph.D. thesis, Applied Physics Series 218, Finnish Academy of Technology, Helsinki (1998), p 69.

[Alm91] A. Almazouzi, J. Bernardini, E.G. Moya, H. Bracht, N.A. Stolwijk and H. Mehrer, J. Appl. Phys. **70**, 1345 (1991).

[Azi01] M.J. Aziz, Mat Sci. Sem. Proc. **4**, 397 (2001).

[Azu03] Y. Azuma, N. Usami, T. Ujihara, K. Fujiwara, G. Sazaki, Y. Murakami and K. Nakajima, J. Crystal Growth **250**, 298 (2003).

[Ben87] A. Benninghoven, F.G. Rüdenauer and H.W. Werner in *Secondary Ion Mass Spectrometry* Volume 86 in series of Chemical Analysis edited by P.J. Elving, H.D. Winefordner and I.M. Kolthoff, John Wiley & Sons, New York (1987).

[Ber81] *Sputtering by Particle Bombardment I,* edited by R. Behrisch, Springer Verlag, Berlin (1981).

[Ber91] *Sputtering by Particle Bombardment III*, edited by R. Behrisch and K. Wittmaack, Springer Verlag, Berlin (1991).

[Bli97] D. Bliss, B. Demczyk, A. Anselmo and J. Bailey, J. Crystal Growth **174**, 187 (1997).

[Boi90] C. Boit and F.L.R. Sittig, Appl. Phys. A **50**, 197 (1990).

[Bon01] J.M. Bonar, A.F.W. Willoughby, A.H. Dan, B.M. McGregor, W. Lerch, D. Loeffelmacher, G.A. Cooke and M.G. Dowsett, J. Mat. Sci. Mat. El. **12**, 219 (2001).

[Bor88] R.J. Borg, G.J. Dienes, *An Introduction to Solid State Diffusion*, Academic Press Inc., New York (1988).

[Bow92] M.D.J. Bowyer, D.G. Ashworth and R. Oven, Sol. Stat. El. **35**, 1151 (1992).

[Bra91] H. Bracht, N.A. Stolwijk and H. Mehrer, Phys. Rev. B **43**, 14465 (1991).

[Bra95] H. Bracht, N.A. Stolwijk and H. Mehrer, Phys. Rev. B **52**, 16542 (1995).

[Bra98] H. Bracht, E.E. Haller and R. Clark-Phelps, Phys. Rev. Lett. **81**, 393 (1998).

[Bro87] G.B. Bronner and J.D. Plummer, J. Appl. Phys **61**, 5286 (1987).

[Bun00] M.M. Bunea and S.T. Dunham, Phys. Rev. B **61**, R2397 (2000).

[Chu78] W.K. Chu, J.W. Mayer and M.A. Nicolet, *Backscattering Spectrometry*, Academic Press, New York (1978)

[Com58] K. Compaan and Y. Haven, Trans. Faraday Soc. **54**, 1498 (1958).

[Cow94] N.E.B. Cowern, P.C. Zalm, P. van der Sluis, D.J. Gravesteijn and W.B. de Boer, Phys. Rev. Lett. **72**, 2585 (1994).

[Cra75] J. Crank, *The mathematics of diffusion*, Clarendon Press, Oxford (1975).

[Dal01]

[Den97] P. Dendooven, Nucl. Instr. and Meth. B **126**, 182 (1997)

[Dis64] J.P. Dismukes, L. Ekstrom and R.J. Paff, J. Phys. Chem. **68**, 3021 (1964).

[Dun95] S.T. Dunham and C.D. Wu, J. Appl. Phys **78** (1995) 2362.

[Egu02] S. Eguchi, J.L. Hoyt, C.W. Leitz and E.A. Fitzgerald, Appl. Phys. Lett. **80**, 1743 (2002).

[Fan96] T.C.W. Fang, T.T. Fang, P.B. Griffin and J.D. Plummer, Appl. Phys. Lett. **68**, 2085 (1996).

[Faz00] A. Fazzio, A. Janotti, A.J.R. da Silva and R. Mota, Phys. Rev. B **61**, R2401 (2000).

[Fis99] R. Fischer, W. Frank and K. Lyutovich, Physica B **273-274**, 598 (1999).

[Fra56] F.C Frank and D. Turnbull, Phys. Rev. **104**, 617 (1956).

[Fra84] W. Frank, U. Gösele, H. Mehrer and A. Seeger in *Diffusion in Crystalline Solids*, Edited by G.E. Murch and A.S. Nowick, Academic Press, Orlando (1984), p 63.

[Fri95] M. Friesel, U. Södervall and W. Gust, J. Appl. Phys. **78**, 5351 (1995).

[Fro95] T. Fromherz, G. Bauer in *Properties of Strained and Relaxed Silicon Germanium,* edited by K. Kasper, INSPEC, London (1995), p 87.

[Fuc95] H.D. Fuchs, W. Walukiewicz, E.E. Haller, W. Dondl, R. Schorer, G. Abstreiter, A.I. Rudnev, A.V. Tikhomirov and V.I. Ozhogin, Phys. Rev. B **51**, 16817 (1995).

[Gie00] A. Giese, H. Bracht, N.A. Stolwijk and D. Baither, Mat. Sci. Eng. B **71**, 160 (2000).

[Gil98] W.P. Gillin and D.J. Dunstan, Comp. Mat. Sci. **11**, 96 (1998).

[Gho71a] R.N. Ghostagore, Phys. Rev. B **3**, 389 (1971).

[Gho71b] R.N. Ghostagore, Phys. Rev. B **3**, 397 (1971).

[Gla77] V.B. Glazman and G.S. Mayken`kaya, Izv. Akad. Nauk. Kuz. SSR, Ser. Fiz. Mat. **15**, 28 (1977).

[Gli55] M. Glickman, Phys. Rev. **100**, 1146 (1955).

[Goe02] S. Goedecker, T. Deutsch and L. Billard, Phys. Rev. Lett. **88**, 235501 (2002).

[Gös80] U. Gösele, W. Frank and A. Seeger, Appl. Phys. **23**, 361 (1980).

[Gös86] U. Gösele, Mater. Res. Soc. Symp. Proc. **59**, 419 (1986).

[Hu78] S.M. Hu, Phys. Stat. Solidi B **60** (1973) 595.

[ICD03] 22th International Conference on Defects in Semiconductors, Conference Proceedings, in print (2003)

[ISO] ISOLDE website: http://isolde.web.ch/ISOLDE.

[Jää01] A. Jääskeläinen, L. Colombo and R. Nieminen, Phys. Rev. B **64**, 233203 (2001).

[Kas75] E. Kasper, H.J. Herzog and H. Kibbel, Appl. Phys. **8**, 199 (1975).

[Kha94] Y.L. Khait and R. Beserman, Phys. Rev. B **50**, 14893 (1994).

[Kri94] P. Kringhoj and R.G. Elliman, Appl. Phys. Lett. **65**, 324 (1994).

[Kri97] P. Kringhoj and A. Nylandsted Larsen, Phys. Rev. B **56**, 6396 (1997).

[Kuo95a] P. Kuo, J.L. Hoyt and J.F. Gibbons, Appl. Phys. Lett **66**, 580 (1995).

[Kuo95b] P. Kuo, J.L. Hoyt and J.F. Gibbons, Mat. Res. Soc. Symp. Proc **379**, 373(1995).

[Mah00] S. Mahajan, Acta. Mater. **48**, 137 (2000).

[Mat78] S. Matsumoto and T. Niimi, J. Electrochem. Soc. **125**, 1307 (1978).

[Maz90] R.G. Mazur and D.H. Dickey, J. Electrochem. Soc. **137**, 679 (1990).

[McD03] F.D. McDaniel,G.V. Ravi Prasad, P. Pelicon and L.J. Mitchell, ISMAS Jubilee Symposium on Mass Spectrometry, Indian Society of Mass Spectrometry, ISMAS-SJS-2003, 247 (2003).

[McV73] G.L. McVay and A.R. DuCharme, J. Appl. Phys **44**, 1409 (1973).

[McV74] G.L. McVay and A.R. DuCharme, Phys. Rev. B **9**, 627 (1974).

[Mee67] W. Meer and D. Pommerrenig, Z. Angew. Phys.**23**, 369 (1967).

[Meh36] R.F. Mehl, Trans. AIME **122**,11 (1936).

[Mes03] A. Mesli and A. Nylandsted Larsen, Nucl. Inst. Methd. B **211**, 80 (2003).

[Mey36] W. Meyer and H. Nedel, Zeitschrift Technische Physik **12**, 588 (1937).

[Mit96] S. Mitha, M. Aziz, D. Schiferl and D.B. Poker, Appl. Phys. Lett. **69**, 922 (1996).

[Mit04] L.J. Mitchell, G.V. Ravi Prasad, P. Pelicon, E.B. Smith and F.D. McDaniel, to be published in Nucl. Inst. Methd. B (2004).

[Mor88] F.F. Morehead, Mat. Res. Symp. Proc. **104**, 99 (1988).

[Mun83] J.N. Mundy and S.J. Rothman, J. Vac. Sci. Techn. A **1**, 74 (1983).

[Nob94] D. Nobili, S. Solmi, A. Parasini, M. Derdour, A. Armigliato and L. Moro, Phys. Rev. B **49**, 2477 (1994).

[Nor97] K. Nordlund and R.S. Averback, Phys. Rev. B **56**, 2421 (1997).

[Nyl96] A. Nylandsted Larsen and P. Kringhoj, Appl. Phys. Lett. **68**, 2684 (1996).

[Nyl00] A. Nylandsted Larsen, Mat. Sci. Eng. B **71**, 6 (2000).

[Pak02] A. Pakfar, Mat. Sci. Eng. B **89**, 225 (2002).

[Pan86] K.C. Pandey, Phys. Rev. Lett. **57**, 2287 (1986).

[Pan97] O. Pankratov, H. Huang, T. Diaz de la Rubia and C. Mailhiot, Phys. Rev. B **56**, 13 172 (1997).

[Pau00] D.J. Paul, Physics World **13**, 27 (2000).

[Peo85] R. People and J.C. Bean, Appl. Phys. Lett. **47**, 322 (1985).

[Peo86] R. People and J.C. Bean, Appl. Phys. Lett. **49**, 229 (1986).

[Pru92] A. Pruijmboom, C.E. Timmering, J.M.L. van Rooij-Mulder, D.J. Gravesteijn, W.B. de Boer, W.J. Kesten, J.W. Slotboom, C.J. Vriezema and R. de Kruif, Micr. El. Ing. **19** (1992) 427.

[Ram03] P. Ramanarayanan and K. Cho, B.M. Clemens, J. Appl. Phys. **94**, 174 (2003).

[Roo81] H.E. Roosendaal in *Sputtering by Particle Bombardment I*, edited by R. Behrisch, Springer Verlag, Berlin (1981), p 219.

[Ros00] C. Rosenblad, M. Kummer, A. Dommann, E. Müller, M. Gusso, L. Tapfer and H. von Känel, Mat. Sci. Eng. B **74**, 113 (2000).

[Rot84] S.J. Rothman in *Diffusion in Crystalline Solids*, Edited by G.E. Murch and A.S. Nowick, Academic Press, Orlando(1984), p 2.

[See68] A. Seeger and K.P. Chik, Phys. Stat. Solidi **29**, 455 (1968).

[Sha90] B.L. Sharma, Def. Diff. Forum **70-71**, 1 (1990).

[Sch49] W. Schockley, Bell Sys. Tech. J. **28**, 436 (1949).

[Sch02] *Impurities and Defects in Group IV Elements IV-IV and III-V Compounds* edited by M. Schulz, Springer-Verlag, Berlin Heidelberg (2002).

[Sed85] T.O. Sedgwick, A.E. Michel, S.A. Cohen, V.R. Deline and G.S. Oehrlein, Appl. Phys. Lett. 47, 848 (1985).

[Siz78] R. Sizmann, J. Nucl. Mat. **69-70**, 386 (1978).

[Sto83] N.A. Stolwijk, B. Schuster, J. Hölzl, H. Mehrer and W. Frank, Physica B **116**, 335 (1983).

[Sto85] A. Stoljwik, W. Frank, J. Hölzl, S.J. Pearton and E.E. Haller, J. Appl. Phys. **57**, 5211 (1985).

[Str01] A. Strohm, S. Matics and W. Frank, Def. Diff. Forum **194-199**, 629 (2001).

[Str02] A. Strohm, Ph. D. Thesis, Max Planck-Institut für Metallforschung und Institut für Theoretische und Angewandte Physik, Universität Stuttgart, Stuttgart (2002).

[Stö39] H. Stöhr, W. Klemm, Z. Anorg. Allg. Chem. **241**, 305 (1939).

[Tan85] T.Y. Tan, U. Gösele, Appl. Phys. A **37**, 1 (1985).

[Tan97] M. Tang, L. Colombo, J. Zhu and T.D. de la Rubia, Phys. Rev. B **55**, 14279 (1997).

[Upp01] S. Uppal, A.F.W. Willoughby, J.M. Bonar, A.G.R. Evans, N.E.B. Cowern, R. Morris and M.G. Dowsett, J. Appl. Phys **90**, 4293 (2001).

[Upp03] S. Uppal, A.F.W. Willoughby, J.M. Bonar, N.E.B. Cowern, R. Morris, M. Bollani and M.G. Dowsett, International Conference on Defects in Semiconductors, Conference Proceedings in print (2003).

[Ura99] A. Ural, P.B. Griffin and J.D. Plummer, Phys. Rev. B **83**, 3454 (1999).

[Ven02] P. Venezuela, G.M. Dalphian, A.J.R. da Silva and A. Fazzio, Phys. Rev. B **65**, 193306 (2002).

[Vos02] T. Voss, A. Strohm, S. Matics, P. Scharwaechter and W. Frank, Z. Metallkd. **93** (2002) 10.

[Vos03] T. Voss, A. Strohm and W. Frank, Z. Metallkd. **94,** 4 (2003).

[Wat81] G.D. Watkins in *Defects in Semiconductors*, edited by J. Narayan and T.Y. Tan, North-Holland, New York (1981), p 21.

[Wat00] G.D. Watkins, Mat. Sci. Sem. Proc. **3**, 227 (2000).

[Web95] J. Weber and M.I. Alonso, Phys Rev. B **40**, 5683 (1995).

[Wer85] M. Werner and H. Mehrer, Phys. Rev. B **6**, 3930 (1985).

[Wol96] J. Wollweber, D. Schulz and W. Schröder, J. Crystal Growth **158**, 404 (1999).

[Yon99] I. Yonega, J. Crystal Growth **198/199**, 404 (1999).

[Yos67] M. Yoshida, K. Saito, Jpn. J. Appl. Phys. **6**, 573 (1967).

[Xie99] Y.H. Xie, Mat. Sci. Eng **25**, 89 (1999).

[Zim92] H. Zimmermann and H. Ryssel, Appl. Phys. A **55**, 121 (1992).

[Zan00] N. Zangenberg, J. Lundsgaard Hansen, J. Fage-Pedersen and A. Nylandsted Larsen, Phys. Rev. Lett **87**, 125901 (2001).

[Zan03] N. Zangenberg, J. Fage-Pedersen, J. Lundsgaard Hansen and A. Nylansted Larsen, J. Appl. Phys. **94**, 3883 (2003).

[Zan03b] N. R. Zangenberg and A. Nylandsted Larsen, International Conference on Defects in Semiconductors, Conference Proceedings in print (2003).